

IN-ORBIT LIFETIME PREDICTION FOR LEO AND HEO BASED ON ORBIT DETERMINATION FROM TLE DATA

A. Águeda ⁽¹⁾, L. Aivar ⁽²⁾, J. Tirado ⁽³⁾, J.C. Dolado ⁽⁴⁾

⁽¹⁾ GMV S.A., Isaac Newton 11, 28760 Tres Cantos, Spain, Email: aagueda@gmv.com

⁽²⁾ GMV S.A., Isaac Newton 11, 28760 Tres Cantos, Spain, Email: laivar@gmv.com

⁽³⁾ GMV S.A., Isaac Newton 11, 28760 Tres Cantos, Spain, Email: jtirado@gmv.com

⁽⁴⁾ CNES, 18 Avenue Édouard Belin 31400 Toulouse, France, Email: Juan-Carlos.DoladoPerez@cnes.fr

ABSTRACT

Objects in Low-Earth Orbits (LEO) and Highly Elliptical Orbits (HEO) are subjected to decay and re-entry into the atmosphere due mainly to the drag force. While being this process the best solution to avoid the proliferation of debris in space and ensure the sustainability of future space activities, it implies a threat to the population on ground. Thus, the prediction of the in-orbit lifetime of an object and the evaluation of the risk on population and ground assets constitutes a crucial task. This paper will concentrate on the first of these tasks.

Unfortunately the lifetime of an object in space is remarkably difficult to predict. This is mainly due to the dependence of the atmospheric drag on a number of uncertain elements such as the density profile and its dependence on the solar activity, the atmospheric conditions, the mass and surface area of the object (very difficult to evaluate), its uncontrolled attitude, etc.

In this paper we will present a method for the prediction of this lifetime based on publicly available Two-Line Elements (TLEs) from the American USSTRATCOM's Joint Space Operations Center (JSpOC). TLEs constitute an excellent source to access routinely orbital information for thousands of objects even though of their reduced and unpredictable accuracy.

Additionally, the implementation of the method on a CNES's Java-based tool will be presented. This tool (OPERA) is executed routinely at CNES to predict the orbital lifetime of a whole catalogue of objects.

1 INTRODUCTION

This paper describes the algorithms implemented for outliers' edition, manoeuvre detection, preliminary area-to-mass ratio estimation and final orbit determination based on the TLE datasets for both LEO and HEO objects. Additionally, the accuracy (estimation error) of the results obtained for known past re-entries will be presented depending on the length of the dataset, and the proximity to the final re-entry and the existing solar activity during the re-entry.

2 SOFTWARE REUSE

OPERA leans on two libraries for the low-level tasks; it mainly uses OREKIT [2] (Orbits Extrapolation KIT) for all the TLE treatment and STELA [3] (Semi-analytic Tool for End of Life Analysis) for the propagation in mean elements.

OREKIT is a free low-level space dynamics library written in Java. It provides basic elements (orbit, dates, attitudes, frames...) and various algorithms to handle them (conversions, analytical and numerical propagation, pointing...).

STELA is a software designed by CNES and developed in cooperation with IMCEE to support the French Space Act. The software allows efficient long-term propagation of LEO, GEO and HEO types orbits based on a semi-analytical method that is much better suited for long term extrapolation than numerical propagation, with no singular equation in eccentricity and inclination.

As the used propagator plays an important role in the orbit determination, a brief description of the STELA propagator in mean elements is presented. The short periods are analytically removed from the equations of motion, so only the middle and long term evolution of the orbital parameters are integrated. The integrator is numerical and it is based on a sixth-order Runge-Kutta method. The elimination of the short period terms allows the use of a very large integration step, reducing significantly the computation time without losing a significant precision on long term (several years) mean evolution. The type of perturbations considered in the propagation model depends on the type of orbit (LEO, GEO or HEO).

STELA can also be used as Java library.

3 ALGORITHMS AND IMPLEMENTATION

This section presents an overview of the whole process developed for OPERA. Besides, a further description of the algorithms used in each part is introduced. OPERA has been developed to be used as a Java library.

Fig. 1 shows the schema of the whole algorithm

developed for OPERA. The first part consists on the TLE filtering (TLE outliers and manoeuvres detection) in order to perform the rest of the process just for the selected data of the selected objects (manoeuvred objects are not considered for the process). Then, this input data is prepared for the orbit determination process, so “real” pseudo-measurements are generated and the initial conditions (state vector and dynamic parameters S_{drag}/m , and S_{SRP}/m when required) are

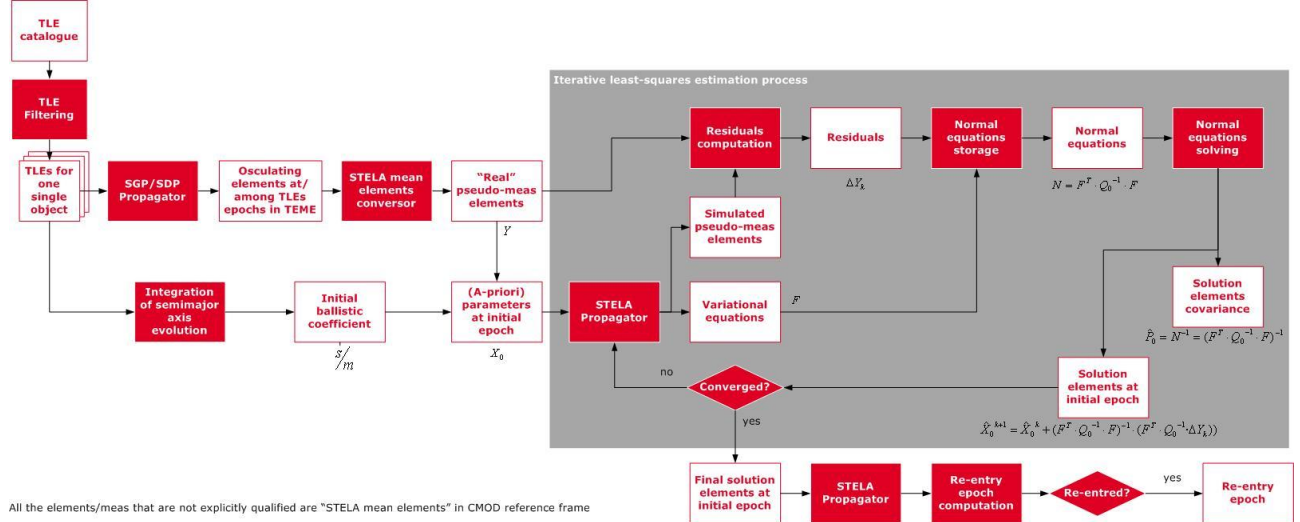


Figure 1: Schema of the re-entry forecasting algorithm

3.1 TLE Outliers Detection

The TLEs are the input data of this algorithm and they are also considered as the measurements of the orbit determination algorithm. Then, it is of key importance to detect and filter any TLE outlier that may disturb the correct convergence of the estimation filter.

The outlier’s detector consists on an iterative least-squares polynomial fitting of each orbital parameter. As no information is available about the uncertainty of the orbital elements of each TLE, and in order to better evaluate the coherence or incoherence of the temporal evolution of the orbital data the orbital elements are expressed in an equinoctial space (1) as their temporal evolution is smoother and thus better suited for outlier detection and filtering in absence of any other information. Moreover, the second and the third parameters are combined, and just the eccentricity evolution is considered.

$$\begin{pmatrix} a \\ e \cos(\omega + \Omega) \\ e \sin(\omega + \Omega) \\ \sin(i/2) \cos(\Omega) \\ \sin(i/2) \sin(\Omega) \\ \Omega + \varpi + M \end{pmatrix} \quad (1)$$

Fig 2 shows the results of the outlier’s detector where

obtained where S_{drag} stands for the mean cross sectional area exposed to drag forces and S_{SRP} stands for the mean cross sectional area surface exposed to the solar radiation pressure, considering an spherical geometry for the space object. Once the initial conditions has been obtained and the observed states filtered, the orbit can be estimated using, in our case, an iterative least square estimation process as shown in Fig. 1 and described in paragraph 3.4.

the blue dots represent the input data from TLEs, the magenta curve corresponds to the fitted polynomial and the red circles are the detected and eliminated outliers. This figure shows an example of the good performance of the outlier’s detector developed as a first step of the process to avoid the insertion of aberrant values in the following steps.

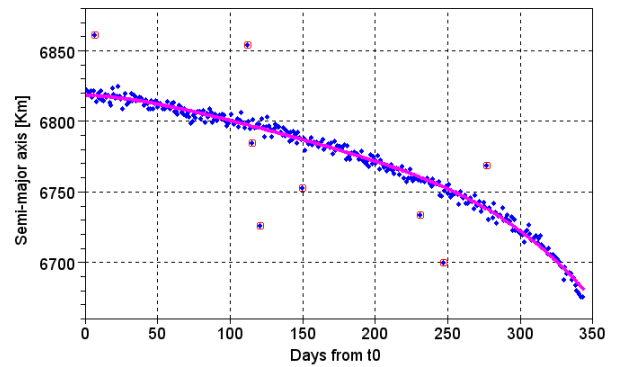


Figure 2: Result of the outlier detection and suppression algorithm on simulated data

It is important to remark that the number of outliers on the space-track TLE sets is relatively low. Usually, most of these outliers appear during the re-entry phases as well as after injection of objects in orbit, where either the few amount of data or the high rate of change of

orbital parameters due mainly to drag, add a significant amount of uncertainty to the orbit determination problem.

3.2 Manoeuvre Detection

OPERA has been defined as a tool to estimate uncontrolled short and middle term re-entry dates. Then, all the manoeuvred objects (i.e. controlled) are filtered and they will not be considered for the process. It is important to filter the manoeuvred objects, because any perturbing acceleration modifying the spacecraft orbital motion will be considered to be of natural origin in the differential correction algorithm. Then, the use of observation affected by orbital manoeuvres that had not been filtered will drive to an aberrant re-entry estimate.

The manoeuvres filtering is done based on TLE data directly, without any propagation. The mean nature of the orbital elements is suitable for manoeuvres detection as any abrupt discontinuity found on the mean orbital evolution will be caused by a manoeuvre. Then, it is only necessary to study the evolution of mean motion and inclination to detect in-plane and out-of plane manoeuvres respectively.

The object will not be considered for the re-entry date estimation if the frequency of the detected manoeuvres is bigger than a user defined value.

3.2.1 In-plane Manoeuvres

In-plane manoeuvres are performed in order to change the evolution of semi-major axis and/or eccentricity. So, it is possible to relate the cause of the manoeuvre ($\frac{\Delta V}{V}$) with its effects ($\frac{\Delta n}{n}$) as (2) states. Then, the term at the right is calculated with the data extracted from the TLE history, and it is considered that a manoeuvre may have taken place if this term is bigger than 10^{-7} . This threshold has been chosen as a trade-off value between the TLEs characteristic noise and the value obtained for known manoeuvres. This criterion is called absolute.

$$\frac{\Delta V}{V} = \frac{-\frac{1}{3} \frac{\Delta n}{n}}{\frac{2}{1-e \cos E} - 1} \quad (2)$$

However, it is not possible to assure that there is a manoeuvre just because this criterion is fulfilled. In fact, lots of “manoeuvres” have been detected with this absolute criterion during the validation campaign which actually did not correspond to true manoeuvres. For that reason, the relative criterion has to be also accomplished to assure that a manoeuvre has been detected. This verification consists in taking a window of 10 TLEs after one detected manoeuvre and calculating the median of the parameter expressed in (2) for this TLE selection. If the value calculated for the first element, the one where the manoeuvre has been detected, is

bigger than 9 times the median, the manoeuvre is confirmed. If there are not enough TLEs to fill the window, this manoeuvre will not be considered. Moreover, considering that the effect of one manoeuvre can be seen in consecutive TLEs, if the manoeuvre is confirmed in consecutive TLEs, just one manoeuvre will be considered.

The values of the thresholds (absolute and relative) and the number of TLEs that the window contains have been defined during the validation campaign. All these values can be re-tuned by the user...

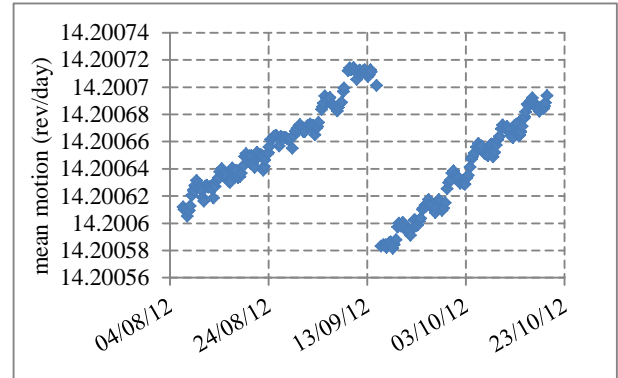


Figure 3: Evolution of SPOT5 mean motion

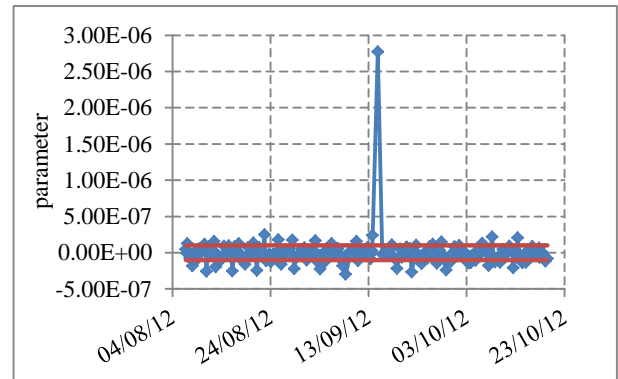


Figure 4: Evolution of the parameter calculated in Eq. (2) to detect the presence of in-plane manoeuvres for SPOT 5 case (Fig. 3)

Fig. 3 shows the evolution of SPOT5 mean motion where it is possible to observe an in-plane manoeuvre around September 14th. Fig. 4 shows the parameter calculated as Eq. (2) states and a peak is found at the same epoch where the manoeuvre was performed. Red lines indicate the thresholds configured for the absolute criteria. It is in the relative criteria when all the points outside the absolute threshold, except the one corresponding to the manoeuvre presented in Fig. 3, are filtered and not considered as possible manoeuvres.

3.2.2 Out-of-plane Manoeuvres

In case that a change in the evolution of the inclination needs to be done, an out-of-plane manoeuvre is performed.

The same process introduced for the in-plane manoeuvres is followed but considering the parameter expressed in (3) instead of the one indicated in (2). After testing with known out-of-plane manoeuvres, a threshold of 10^{-4} is considered for the absolute criteria and a limit value of 8 times the median of the 10 TLEs window is fixed for the relative criteria. These selected values are also chosen as trade-off values between the noise of TLEs and the evolution of the parameters for the objects really manoeuvred.

$$\frac{\Delta V}{V} = \Delta i \quad (3)$$

As in the previous case, if manoeuvres are detected with the relative filter in consecutive TLEs, only one will be considered as the manoeuvre may present its effect in consecutive TLEs.

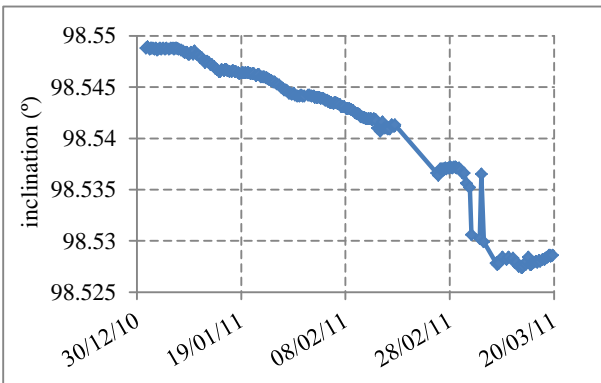


Figure 5: Evolution of ERS2 inclination

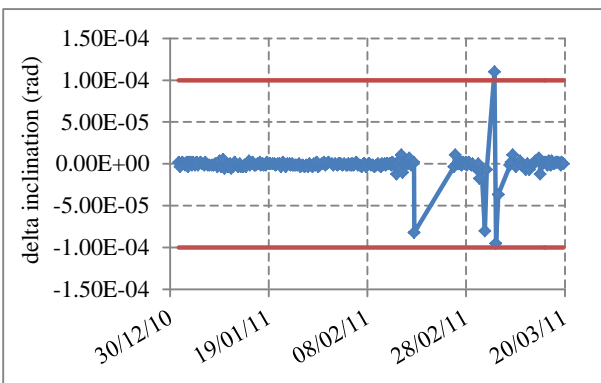


Figure 6: Delta inclination to detect the presence of out-of-plane manoeuvres

Fig. 5 shows the evolution of ERS2 inclination during 80 days including an out-of-plane manoeuvre around March 5th. Fig. 6 depicts the evolution of the delta

inclination, parameter used to detect out-of-plane manoeuvres, where the red lines represent the thresholds configured for the absolute criterion. The only point that exceeds these thresholds corresponds to the out-of-plane manoeuvre presented in Fig. 5.

3.3 Preliminary Area-to-Mass Ratio Estimation

In order to linearize the problem of orbit estimation around an initial condition that assures the convergence of the orbit determination process, it is necessary to estimate an initial condition close enough from the unknown real orbit to guarantee the linearity of the estimation problem. Input TLEs contain information accurate enough to initialize the state vector, but there is no information available to initialize the dynamic parameters, which are of key importance to describe the effect of perturbation on the motion of the satellite.

Therefore, these dynamic parameters, mainly S_{drag}/m , and S_{SRP}/m , need to be estimated to initialize the orbit determination process.

So as to simplify this process, it is considered that the mean evolution of the semi-major axis with time is exclusively due to the drag perturbation acceleration. Hence, the area-to-mass ratio estimated corresponds to S_{drag}/m . If an HEO object is being analysed, this area-to-mass ratio value is also used to initialize the S_{SRP}/m .

Given that only uncontrolled objects are taken into account in this process, it is possible to consider that they are randomly tumbling. Consequently, the satellite geometry may be assimilated to a sphere whose cross sectional area is equal to the drag surface.

As STELA does in its internal propagation, the drag coefficient (C_x) is taken from a curve established in [4]. This curve expresses the drag coefficient for a sphere with respect to the altitude.

By the numerical integration of the second term of (4), it is possible to obtain a first guess of the area-to-mass ratio; hereafter called a-priori area-to-mass ratio.

$$\frac{1}{a(t_0)} - \frac{1}{a(t)} = -\frac{1}{\mu} \frac{S_{drag}}{m} \int_{t_0}^t \rho C_x V^3 dt \quad (4)$$

However, this method does not always give results accurate enough to initialize the process, mostly for HEO objects as the solar radiation pressure perturbing acceleration may be of the same order of magnitude or even bigger than the drag perturbing acceleration. So as to refine this initial estimation of the area-to-mass ratio, a bisection method algorithm has been developed. This method consists on the minimization of the L1-norm of the difference between the input semi-major axis (taken from TLEs) and the simulated one at the end of the

propagation. The a-priori area-to-mass ratio is used to start this iterative process. The convergence of this refinement method is reached when the L1-norm difference relative to the semi-major axis is smaller than 0.005%; a value that can be configured by the user.

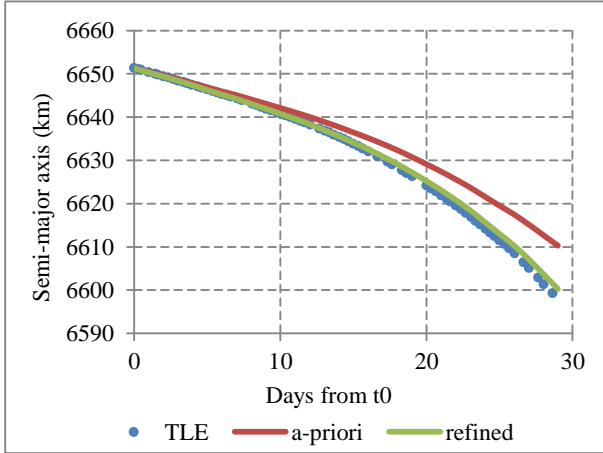


Figure 7: Observed mean semi-major axis evolution from TLEs (blue dots), simulated mean semi-major axis evolution using the a-priori area-to-mass ratio (red curve) and using the refined area-to-mass ratio (green curve) for a LEO simulation

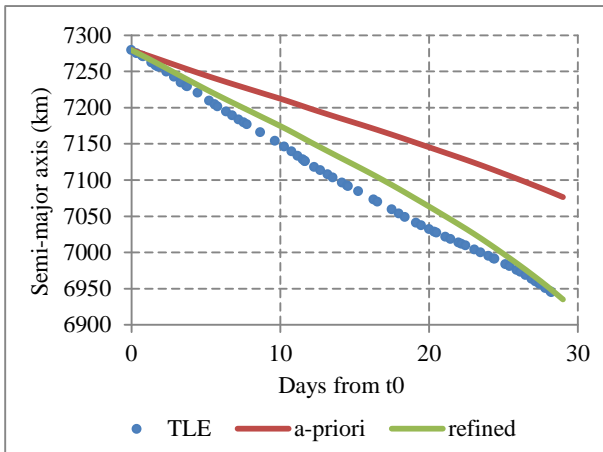


Figure 8: Observed mean semi-major axis evolution from TLEs (blue dots), simulated mean semi-major axis evolution using the a-priori area-to-mass ratio (red curve) and using the refined area-to-mass ratio (green curve) for a HEO simulation

It is possible to see in Fig 7 and 8 how the evolution obtained with the a-priori area-to-mass ratio (red) does not fit properly enough the evolution presented by the measurements (TLEs in blue). However, the evolution obtained with the refined area-to-mass ratio (green) is accurate enough to start the orbit determination process.

3.4 Orbit Determination

Once that accurate enough initial conditions have been

calculated, it is possible to linearize the formulation of the orbit determination problem using a Taylor expansion as (5) states. y_m stands for the measurements used for the determination, x_n for the initial state vector to be determined, F_m is the transition matrix, ε represents the errors of every measurement, n is the number of estimated parameters and m is the total number of observations ($m > n$)

$$y_m = F_m x_n + \varepsilon \quad (5)$$

The least-squares method is intended to optimize the squares sum of the residuals estimation.

The considered measurements are expressed in keplerian components and it is possible to use the information coming from just position or both position and velocity for the orbit determination process. Given the source (taken from the USSTRATCOM's catalogue) and the nature (keplerian elements where the order of magnitude of position components is completely different from the one for velocity components) of the measurements, an a-priori weighting matrix of the measurements is added to the process to achieve a better conditioning when inverting F .

Theoretical measurements, that are used to calculate the residuals w.r.t. the real measurements, are obtained with a STELA propagation starting from the initial state vector. If real and theoretical measurement's epochs do not coincide, an 8th order Lagrange interpolation is performed to obtain the theoretical measurement at the same epoch as the real measurement and hence calculate the residual. Considering that STELA propagates in mean elements with an integration step of the same order of magnitude that the orbital period, the mean argument of latitude does not represent the real orbital position of the space object at the date of release of the state vector. Therefore for the orbit determination process, and in order to guarantee the linearity of the problem, the theoretical AOL (Argument of Latitude) is forced to be the same than the observed one. An additional Gaussian noise is added to the theoretical AOL in order to not over constraint the solution. .

STELA also gives the transition matrix (partial derivatives) as output, which can be directly used for the orbit determination if the epochs fit with the epochs of the real measurements. Otherwise, a Lagrange interpolation of the partial derivatives needs to be done.

Finally, (6) expresses the orbit determination problem including all the assumption here mentioned.

$$\hat{X}_0^{k+1} = \hat{X}_0^k + (F^T Q_0^{-1} F)^{-1} (F^T Q_0^{-1} \Delta Y^k) \quad (6)$$

This iterative process will end when one of the convergence criteria takes place.

Once the OD is finished, the initial state is determined and it is propagated with STELA until re-entry, in order

to provide the re-entry date to the user.

3.4.1 Difficulties presented in the orbit determination approach

Several problems arise when trying to perform non-linear orbit determination from external catalogues, in particular from the public USSTRATCOM catalogue.

Data sparse distribution. The frequency of TLE sets for an object is not constant; the distribution of input data is particular for every simulation. Thus, it is of key importance to develop an orbit determination algorithm capable to handle these different input conditions.

Existence of non-observable parameters. [5] states that TLE epochs coincide with the ascending node prior to the last observation. As TLEs are considered the measurements of the developed orbit determination process, data from the same orbital point is always taken into consideration. Consequently, the difficulty to observe some parameters such as eccentricity will impact the accuracy of the estimated vector.

Computational time. Considering the large catalogue of active LEO and HEO objects whose re-entry date needs to be calculated, it is important to optimize the computational time for each individual orbit determination. Using a mean elements approach for the orbit determination process enables a considerable reduction in the needed computational time.

4 RESULTS

This section presents the results obtained with OPERA for satellites that have already re-entered, thus a real re-entry date is available to evaluate the quality of the estimated re-entry dates.

Furthermore, most of the results here presented have been produced and used for operational short and middle term re-entry prediction at CNES. Such middle term re-entry is of key importance to plan the on-ground space surveillance network operations, as it has to be scheduled several days in advance of the re-entry date.

To a better understanding of the figures to come, re-entry estimations with OPERA are done up to one week prior to the estimated re-entry date. From one week to the effective re-entry date, more accurate radar and optical measurements are used to estimate the re-entry date.

Real solar activity is considered up to the epoch of the last TLE considered for the process. Then, the orbit determination is done taking into consideration real solar activity information. From this epoch on, propagation until re-entry, predicted solar activity is considered.

Fig. 9 shows the evolution of the estimated re-entry dates for COSMOS 1484. This LEO object re-entered

on January 28th 2013, as the dotted red line highlights.

These re-entry dates have been calculated using a TLE catalogue of 30 days from the date indicated in the x axis of Fig. 9. Whereas blue diamonds represent the estimated re-entry date with OPERA (y-axis) for every initial state (x-axis), grey diamonds represent the prediction uncertainty bounds estimated for every obtained date. The uncertainty bounds are calculated as a +/-10% of the difference between the estimated re-entry date and the epoch of the initial state vector used for the orbit determination.

The first simulation is done three months before the re-entry and the error obtained in the estimated date is 20 days (i.e.16% estimation error), so out of the 10% estimated uncertainty bounds. Although this estimated date is not as accurate as it is supposed to be, a re-entry warning appears denoting that close attention should be paid to this object.

Closer the data from re-entry is used; more precise the estimation of the re-entry date will be. Determining the state vector 2 months previous to the effective re-entry date, it is already possible to estimate a re-entry date whose bounds include the real re-entry date. From here on, although the uncertainties bounds become smaller, the real re-entry date is always included in them.

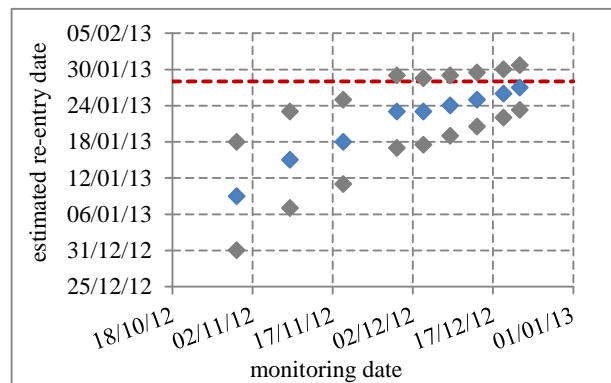


Figure 9: Evolution of the estimated re-entry date for COSMOS 1484 using a TLE catalogue of 30 days

An important parameter to take into account in these simulations is the length of the TLE catalogue considered for the prediction process. The duration should be long enough to contain enough measurements, so enough information, to characterize the whole dynamic of the orbit in order to make possible an accurate enough orbit determination process. An idea of the sensitivity of the results to the amount of data used for the orbit determination is shown in Fig. 10 where the same previous scenario has been simulated, but considering a shorter TLE time series (i.e. 10 days of TLEs instead of 30). Reducing the amount of data used for the orbit determination penalizes the accuracy of the estimated orbit; hence the obtained re-entry dates are further from the real one, in comparison with the

previous scenario predictions. Based on experience, a 30-day time span of measurements (i.e. TLE data) has been found as a good trade-off for LEO objects between accuracy of the estimated orbit and computation time.

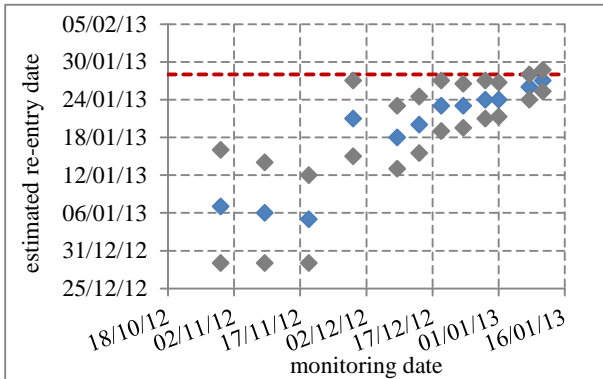


Figure 10: Evolution of the estimated re-entry date for COSMOS 1484 using a TLE catalogue of 10 days

Performances of OPERA have also been tested with a HEO object. Fig. 11 shows the evolution of the estimated re-entry dates for BREEZE-M DEB (NORAD id 38951). As the red dotted line of the next figure depicts, this objet re-entered on February 25th 2013.

A 20-day TLE history from the date indicated in the x axis has been used in these simulations. As in the previous case, the uncertainty bound correspond to the +/-10% of the difference between the estimated re-entry date and the epoch of the initial state vector used for the orbit determination.

Comparing to the results obtained for the LEO object, the convergence to the real re-entry date is slower for the HEO object. Nevertheless, the convergence is reached too.

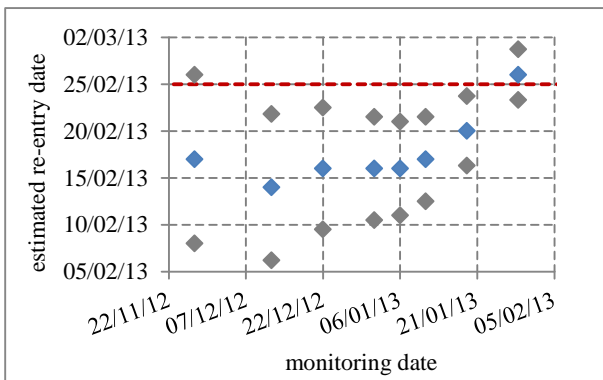


Figure 11: Evolution of the estimated re-entry date for BREEZE-M DEB using a TLE catalogue of 20 days

5 CONCLUSIONS

This paper has presented the development and performances of OPERA. A whole process of orbit determination and input data preparation has been

developed in order to estimate the re-entry date for space objects included in the TLE catalogue.

Despite the used data (USSTRATCOM public TLE) is not the most precise input, but the only publicly available, a satisfactory approach and treatment have been developed in order to perform short and middle term re-entry forecasting. On this approach, TLE are considered as the observations for the orbit determination process. The obtained results strongly depend on the quality of the inputs used (TLE quality, duration, frequency...), but usually OPERA is able to predict the re-entry date with enough accuracy and soon enough to plan the necessary space surveillance campaigns, required to the improvement of the re-entry date prediction.

Besides, it should be mentioned that not only the final estimated re-entry date is important, but also all the intermediate results (detected manoeuvres, a-priori area-to-mass ratio...) are attractive and very useful results of this tool. Because of the good performances found from the developed algorithms for these purposes, these intermediate results can provide extra functionality. For example, it is possible to calculate the initial area-to-mass ratio with OPERA and use it to initialize the osculating orbit determination performed with space surveillance network radar and optical measurements. Or even, to take advantage of the manoeuvres detection algorithm to perform an analysis of the state of the objects' catalogue (e.g. manoeuvring objects ...). Thanks to the re-definition of OPERA's architecture from a stand-alone tool to a Java library, the user can take advantage of all the functionalities of OPERA, in addition of being able to perform short and middle term re-entry predictions from TLE data. .

6 REFERENCES

1. Dolado-Perez, J.C, Aivar Garcia, L., Águeda Maté, A., Hédon, A., Short and Middle Term Uncontrolled Re-Entry Monitoring Using Public Space Debris Catalogues, Proceedings of the AIAA/AAS Astrodynamics Specialist Conference – August 2012
2. <https://www.orekit.org/forge/projects/orekit/wiki/Overview>
3. Fraysse, H., Morand, V., Le Fevre, C., Deleflie, F., Wailliez, S., Lamy, A., Martin, T., Perot, E., Long term orbit propagation techniques developed in the frame of the French Space Act, Proceedings of the 22nd ISSFD- 2011
4. CNES, STELA User's Guide. v.2.4.0, December 2012
5. David A. Vallado, Fundamentals of Astrodynamics and Applications, 3rd ed., Microcosm Press, 2007